MORPHOLOGY AND TECTONICS OF EAST CANDOR CHASMA, VALLES MARINERIS (MARS), AND CORRELATION WITH MINERALOGY. L. Le Deit[1], D. Mège[1], O. Bourgeois[1], S. Le Mouélic[1], C. Sotin[1], E. Hauber[2], N. Mangold[3], J.-P. Bibring[4], [1]Laboratoire de Planétologie et Géodynamique UMR-CNRS 6112, Université de Nantes, Faculté des Sciences et Techniques, 2 chemin de la Houssinière BP 92208, 44322 Nantes Cedex 3, France (laetitia.ledeit@univ-nantes.fr), [2]Institute of Planetary Research, German Aerospace Center (DLR), Berlin, Germany, [3]Orsay-Terre, FRE2566, CNRS et Université Paris-Sud, Bat. 509, 91405 ORSAY Cedex, France [4]Institut d'Astrophysique Spatiale, Université Paris 11, Bâtiment 121, 91405 Orsay Campus, France.

Introduction: East Candor Chasma is one of the large Valles Marineris chasmata (*Figure 1*). It is bounded by walls more than 6 km high displaying the initial spur and gully morphology, locally reworked by mass wasting processes [1]. The floor is covered by landslide deposits, layered deposits (Interior Layered Deposits -ILDs-), and other sedimentary or volcano-sedimentary units [2, 3]. Aeolian morphologies are common and include dunes, aeolian flutes, and yardangs. Erosion has preferentially removed the ILDs in the northern part of the chasma. In this study, we analyse MOLA DEM, HRSC, THEMIS and MOC images in order to characterize the morphology and tectonics of the area. We have also used OMEGA/Mars Express hyperspectral data to complete our analysis with compositional information.

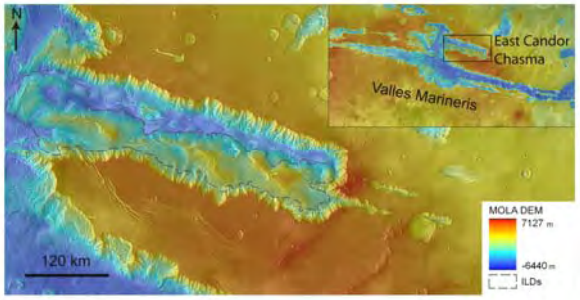

Figure 1: East Candor Chasma region (63.5°W-72°W, 5°S-9°S). MOLA topographic map overlapping a mosaic of THEMIS IR images. ILDs are surrounded by the dashed line.

Datasets: The gridded 128 pixels/degree Mars Orbiter Laser Altimeter (MOLA) DEM provides the global topographic framework with a relative vertical accuracy of ~1 m [4] and a horizontal resolution of 463 m between tracks at the Valles Marineris latitude.

The High Resolution Stereo Camera (HRSC) onboard Mars Express provides high (12.5-30 m/pixel) spatial resolution panchromatic images, colour images at 100 m per pixel and DEMs with a lateral resolution of about 200 m per pixel [5]. In this study, we have mainly used the nadir panchromatic images.

Daytime and night-time infrared Thermal Emission Imaging System (THEMIS) data [6] have been useful for studying geomorphology and thermal emissivity of the surface, respectively. Thermal inertia data inform on surface material ability to retain the heat accumulated during daytime, and is used to identify rock induration contrasts. For instance, weakly indurated aeolian deposits are characterized by low thermal inertia, whereas outcrops of fresh competent rocks are characterized by high thermal inertia [7]. Infrared images have a spatial resolution of 100 m/pixel. Visible THEMIS images (18 m/pixel) have been used to interpret the geomorphology at a scale intermediate between THEMIS IR and HRSC, and MOC.

With a spatial resolution as fine as 1.4 m/pixel [8], the Mars Observer Camera (MOC) images have been used to constrain the geomorphology of specific small areas in detail.

Methodology: In order to facilitate their analysis, these datasets have been combined into a geographic information system using the Mars 2000 geographic coordinate system available in ArcGIS.

The combined data have been used to analyse geomorphological and structural features in order to constrain the evolution of the chasma. OMEGA data analysis provide insights as to their mineralogy, and help characterize their history.

Preliminary results: The first observed step in the evolution of East Candor Chasma is tectonic opening and erosion in the form of spur and gully over most of the wall slopes. The chasma is composed of horsts and grabens, the border faults of which are subparallel to the main trend of the chasma (N105E).

At least two sequences of chasma infilling are observed, the second one being the ILDs, which have covered the whole chasma up to the plateau level.

Chasma infilling was followed by a period of intense erosion and partial exhumation of earlier morphologies, such as the spurs and gullies. This period was associated with minor tectonic activity that decreased the chasma base level and resulted in spur and gully hanging on the northern chasma wall, as reported in [1].

Correlation with OMEGA compositional information: Ferric oxides are a good clue to constrain the role played by water in the chasma history. We performed analysis of OMEGA data using several methods in order to detect and map ferric oxides in East Candor Chasma with a high confidence level [9, 10]. We have defined two different confidence levels in our distribution map of ferric oxides, depending on the quality and

spatial resolution of the available observations. The most robust detections are indicated in orange and areas where the ferric oxide detection still has to be confirmed with new data sets are in blue on *Figure 2*.

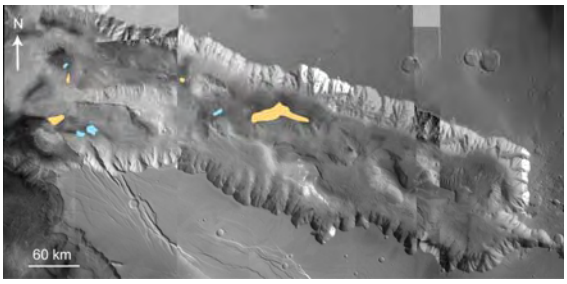

Figure 2: Distribution map of ferric oxides (marked in orange where the level of confidence is high) in East Candor Chasma (63.5°W-72°W, 5°S-9°S) obtained with a detailed study of OMEGA spectra, superimposed on a mosaic of HRSC images. The sites possibly enriched in ferric oxides are in blue.

According to TES measurements [11], thermal inertia of the ferric oxide-rich sites ranges from 277 SI to 643 SI (485 SI on average). We infer that these areas do not correspond to dusty surfaces and that this type of strong ferric signature detected by OMEGA does not correspond to the one due to atmospheric oxidation.

Ferric oxides in East Candor Chasma are distributed in isolated areas. MOLA altimetry indicates that the oxides are preferentially located in topographic lows. THEMIS, HRSC and MOC images show that the ferric oxides are systematically correlated with superficial deposits of low albedo, at the foot of, or over the ILDs. The spatial distribution of ferric oxides in regard with ILDs suggests that they are genetically linked. A remobilization of ferric oxides from the ILDs could explain their accumulation around the ILDs.

We suggest the following formation scenario of ferric oxides in East Candor Chasma (*Figure 3*). First, the chasma would have formed by tectonic processes. In a plausible mode of emplacement, the actual floor materials would have formed at that time and would have been exhumed later (Stage 0). Then, the canyon would have been filled in by ILDs. They consist of light-toned material of volcanic or sedimentary origin, deposited in a body of water, possibly covered by ice [12]. They would contain weathered mafic grains, kieserite (Mg-rich sulfate), and polyhydrated sulfates (Mg- and/or Fe-rich sulfates) [13] (Stage 1). The groundwater recharge with an acid and/or oxidizing water enriched in ferric iron would have implied the in situ precipitation of ferric oxides concretions [14]. The groundwater enrichment in iron may have resulted from dissolution of Fe-rich sulfates [15] (Stage 2). Aeolian ILD erosion would have then produced accumulations of ferric-rich deposits in topographic lows (Stage 3).

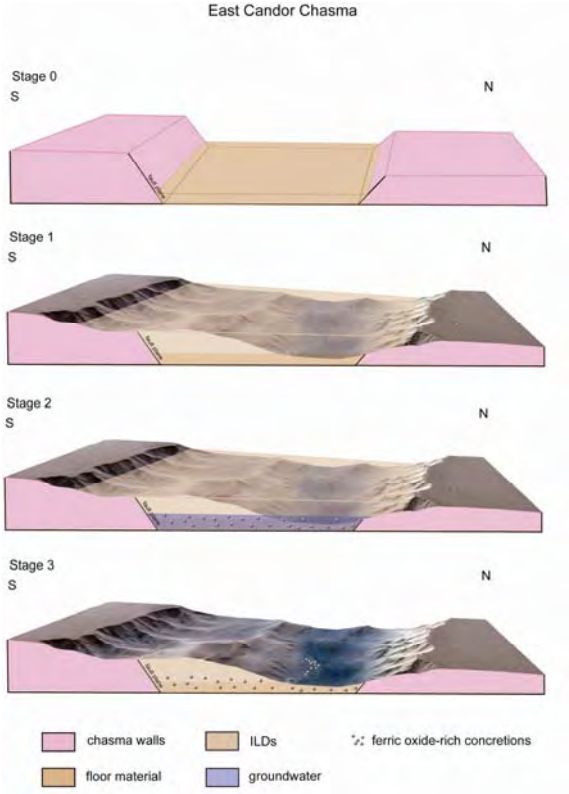

Figure 3: Ferric oxide formation scenario in East Candor Chasma. ***Stage 0:*** *Chasma formation by tectonic processes. Formation of the floor materials.* ***Stage 1:*** *Canyon filled in by ILDs.* ***Stage 2:*** *Groundwater recharge with an acid and/or oxidizing water enriched in ferric iron. In situ precipitation of ferric oxides concretions.* ***Stage 3:*** *Aeolian ILD erosion producing accumulations of ferric-rich deposits in topographic lows.*

Perspectives: The final results and conclusions of this study will be compared to earlier scenarios and models of Candor Chasma evolution [16, 17, 18].

References: [1] Peulvast J.- P.et al. (2001) *Geomorph., 37,* 329-352. [2] Lucchitta B. K.et al. (1992) *Mars*, Univ. of Arizona, Tucson. [3] Quantin C. et al. (2004) *Icarus*, *172*, 555-572. [4] Smith D.E. et al. (2001) *JGR*, *106*, 23,689-23,722. [5] Neukum G. and R. Jaumann R. (2004) *ESA SP-1240.* [6] Christensen P. et al. (2004) *Science*, *306*, 1733-1739. [7] Mellon M.T.et al. (2000) *Icarus*, *148*, 437–455. [8] Malin M.C. et al. (1992) *JGR*, *97*, E5, 7699-7718. [9] Le Deit L. (2006) *LPSXXXVII*, Abstract #2115. [10] Le Deit et al. (2006) *EPSC2006-A-00597*. [11] Putzig N. E. et al. (2005) *Icarus*, *173*, 325–341. [12] Nedell, S. S. and Squyres S.W. (1987) *MECA Symp. on Mars*, 88-90. [13] Gendrin A. et al. (2005) *Science*, *307*, 1587-1591. [14] McLennan S.M.et al. (2005) *EPSL*, *240*, 95–121. [15] Squyres S. W. and Knoll A. H. (2005) *EPSL*, *240*, 1–10. [16] Schultz R. A. (1995) P&SS, 43 1561-1566. [17] Mège D. and Masson P. (1996) P&SS, 44, 8, 749-782. [18] Schultz R.A.(1998) P&SS, 46, 827-834.